

# Dilemma of diagnosing thoracic sarcoidosis in tuberculosis-endemic regions: An imaging-based approach. Part 2

Ashu S Bhalla, A Das, P Naranje, A Goyal, R Guleria<sup>1</sup>, Gopi C Khilnani<sup>1</sup>

Departments of Radiodiagnosis, <sup>1</sup>Pulmonary Medicine and Sleep Disorders, All India Institute of Medical Sciences, New Delhi, India

**Correspondence:** Dr. Ashu S Bhalla, Department of Radiodiagnosis, All India Institute of Medical Sciences, New Delhi - 110 029, India.  
E-mail: ashubhalla1@yahoo.com

## Abstract

The second part of the review discusses the role of different existing imaging modalities in the evaluation of thoracic sarcoidosis, including chest radiograph, computed tomography, magnetic resonance imaging, endobronchial ultrasound, and positron emission tomography. While summarizing the advantages and pitfalls of each imaging modality, the authors propose imaging recommendations and an algorithm to be followed in the evaluation of clinically suspected case of sarcoidosis in tuberculosis-endemic regions.

**Key words:** Magnetic resonance imaging; multidetector computed tomography; radiograph; sarcoidosis; tuberculosis

## Imaging Modalities

The second part of the review deals with choosing and planning optimum imaging modality in clinical scenario of sarcoidosis versus tuberculosis (TB). An imaging algorithm to the effect has also been proposed.

### Chest radiograph

Frontal or postero-anterior (PA) chest radiograph (CXR) is usually the first imaging investigation ordered by the physician as a part of the diagnostic workup for sarcoidosis. In fact, bilateral hilar lymphadenopathy on CXR has been described as characteristic for sarcoidosis in an asymptomatic patient or in conjunction with features of Löfgren syndrome, i.e., erythema nodosum, fever,

and arthralgia. Moreover, the earliest staging system for sarcoidosis described by Siltzbach was based on the findings on CXR and has still remained the most widely used system mainly because of its immense prognostic significance.<sup>[1]</sup> The Siltzbach staging system incorporates five stages of the disease<sup>[2]</sup> with increasing stage being associated with decline of pulmonary function culminating in pulmonary fibrosis. Stage 0 corresponds to normal appearance on CXR; stage 1 with only lymphadenopathy; stage 2 with lymphadenopathy and parenchymal lung disease; stage 3 involves parenchymal lung disease only; and stage 4 with fibrosis. CXR may also be used for routine follow-up of patients with pulmonary sarcoidosis to assess changes in parenchymal and nodal disease with low radiation exposure.<sup>[3]</sup>

### Access this article online

#### Quick Response Code:



**Website:**  
www.ijri.org

**DOI:**  
10.4103/ijri.IJRI\_201\_17

This is an open access article distributed under the terms of the Creative Commons Attribution-NonCommercial-ShareAlike 3.0 License, which allows others to remix, tweak, and build upon the work non-commercially, as long as the author is credited and the new creations are licensed under the identical terms.

**For reprints contact:** reprints@medknow.com

**Cite this article as:** Bhalla AS, Das A, Naranje P, Goyal A, Guleria R, Khilnani GC. Dilemma of diagnosing thoracic sarcoidosis in tuberculosis-endemic regions: An imaging-based approach. Part 2. Indian J Radiol Imaging 2017;27:380-8.

CXR-PA forms an important tool in the diagnostic algorithm for suspected TB in population. Findings on CXR which are highly suggestive (HS) of TB include unilateral hilar/paratracheal lymphadenopathy with or without parenchymal lesions, miliary nodules, and fibro-cavitary lesions.<sup>[4]</sup> In adults also, CXR-PA is an important component of diagnostic algorithm for TB in national TB control programs. CXR findings such as consolidation/air-space involvement with ipsilateral lymphadenopathy, thick-walled cavities, and empyema are HS of TB.<sup>[5]</sup> However, radiographic features such as mediastinal and/or hilar lymphadenopathy, parenchymal nodules, and fibrosis are nonspecific (NS) and may be seen in sarcoidosis or TB.

Though CXR with concordant microbiology can suffice for the diagnosis of TB, the same may not be applicable to suspected cases of sarcoidosis, especially in TB-endemic regions if administration of steroid is being planned. Hence, exclusion of TB in patients presenting with mediastinal lymphadenopathy on CXR becomes imperative before initiation of treatment, thereby underlining the role of supplementary imaging, i.e., computed tomography (CT) scan of thorax [Figure 1].

**Computed tomography**

High-resolution CT (HRCT) has proven to have better efficacy in assessing subtle parenchymal changes, even in early stages of sarcoidosis which may go unnoticed on CXR-PA. Recommended indications of CT in sarcoidosis include atypical clinical manifestations or unusual CXR findings, normal CXR with clinical suspicion of sarcoidosis, detection of complications including pulmonary hypertension, mycetoma formation, airway involvement, and as a pre-transplant workup for end-stage pulmonary fibrosis.<sup>[3]</sup> HRCT has been found to be particularly useful in differentiation of active inflammation from fibrosis, a question of immense clinical and prognostic significance. In cases with atypical radiographic or clinical manifestations, findings on HRCT may help in solving the dilemma by demonstrating characteristic findings.<sup>[6]</sup> HRCT also suffices

for follow-up in patients with equivocal radiographic findings, in correlation with pulmonary functions test (PFT).

Although administration of intravenous (IV) contrast is not routinely recommended in sarcoidosis, it may aid in better depiction of mediastinal lymphadenopathy and in patients with vascular complications such as massive hemoptysis or pulmonary hypertension.<sup>[7]</sup> IV contrast administration is especially helpful in differentiation of sarcoidosis from TB by detection of intranodal necrosis and mapping of the lymph nodal stations. Thus, in endemic regions, contrast enhanced CT (CECT) chest would have to be performed in all suspected cases of sarcoidosis with nodal involvement on CXR to exclude TB [Figure 1].

Indications of CT in TB include detection of radiographically occult disease, evaluation of mediastinal lymph nodes, assessing disease activity, evaluating complications and may aid in differentiation among the etiologies of pneumonia. Moreover, CT findings can help suggest the diagnosis of TB in sputum-negative patients and may permit empirical initiation of anti-TB treatment until the time culture results are obtained.

The role of CT in routine follow-up of sarcoidosis patients is not well defined mainly because of the attendant higher radiation exposure and the relatively younger patient age

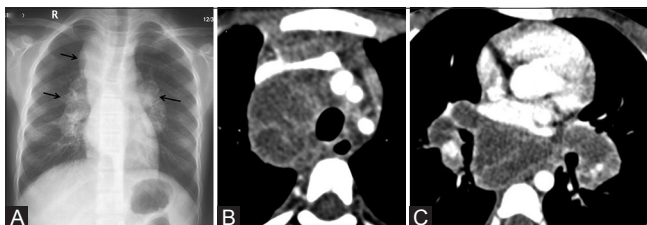


**Figure 1 (A-C):** Discriminatory role of CECT thorax in excluding TB in patients with mediastinal lymphadenopathy on CXR. (A) CXR of 21-year-old boy who presented with fever and weight loss shows right paratracheal and bilateral hilar lymphadenopathy (solid arrow). (B and C, same patient as Figure 2 of part 1) Conglomerate necrotic mediastinal and hilar lymphadenopathy with rim enhancement suggestive of TB. The patient was subsequently started on anti-tubercular therapy

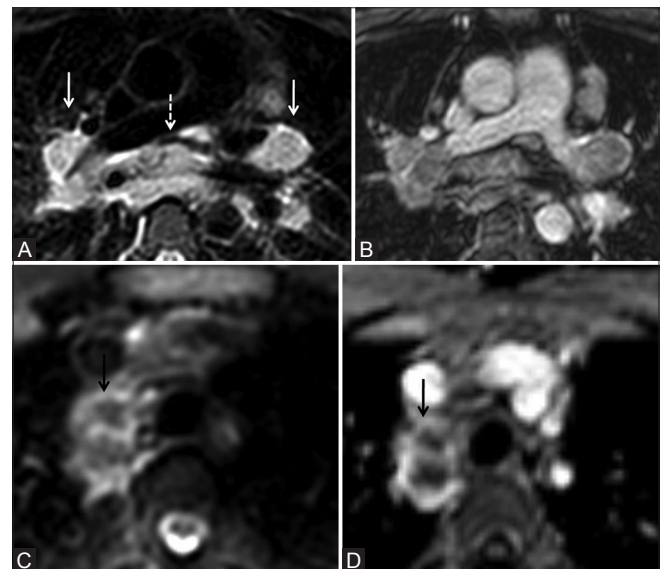


**Figure 2 (A-D):** Role of MRI in evaluation of mediastinal lymphadenopathy in suspected case of sarcoidosis/TB. (A) 40-year-old man with sarcoidosis. Axial T2 FS MR image shows enlarged discrete bilateral hilar (solid arrow) and subcarinal lymph nodes (dashed arrow) showing heterogeneously hyperintense signal. No internal necrosis. (B) Axial post gadolinium T1 FS image shows mild heterogeneous enhancement. (C) 18-year-old girl with lymph nodal tuberculosis. Axial T2 FS image shows conglomerate necrotic right paratracheal lymphadenopathy showing hypointense core suggestive of caseous necrosis and hyperintense rim (black arrow). (D) Axial post gadolinium T1 FS image shows rim enhancement in lymph nodes similar to CECT (black arrow)

**Table 1: Suggested MR sequences for evaluation of lymph nodes and lung parenchyma (our experience)<sup>[11,12,14]</sup>**

Sequence	Orientation	Respiration	TR* (ms)	TE† (ms)	SL‡ (mm)	TA§ (min)	Flip angle (degree)	Voxel size (mm)	Matrix	FOV¶ (mm)	Parallel imaging (acceleration factor)	Fold over direction	NSA**
HASTE††	Coronal	Breath-hold	2000	150	5	4.12	90	1.5×1.8	280×229	420×420	4	RL	2
STIR‡‡	Coronal	Triggered	875	60	5	4.12	-	1.5×1.7	280×247	420×420	3	RL	2
	Axial	Triggered	1235	60	5	5.36	-	1.5×1.8	280×195	420×350	3	AP	2
T2W MV§§ fat suppressed	Axial	Triggered	3366	80	5	3.11	90	1.8×1.8	176×176	350×350	-	-	1
BTfE/SSFP***	Coronal	Free breathing	2.9	1.45	5	2.05	90	1.5×1.7	280×248	420×420	1.5	RL	1
	Axial	Free breathing	2.7	1.3	5	2.47	90	1.5×1.5	250×200	375×300	-	AP	1
T1 DIXON (all)	Axial	Inspiration. Breath-hold	5.9	1.8/4	2.5	13 sec	15	2.2×2.2	160×176	350×380	5	AP	1
DWI††† (b=0, 400 and 800 sec/mm <sup>2</sup> )	Axial	Respiratory navigation - free breathing	4103	67	5	3.41	-	2.75×2.75	136×134	375×375	2	AP	2
T1 DIXON (water only/ fat saturation)	Axial	Breath-hold	5.9	4	2.5	13 sec	15	2×2	176×190	350×380	4	AP	1

\*TR: Repetition time, †TE: Echo time, ‡SL: Slice thickness, §TA: Time to acquisition, ¶FOV: Field of view, \*\*NSA: Number of signal averages, ††HASTE: Half-Fourier acquisition single-shot turbo Spin-Echo, †††STIR: Short tau inversion recovery, §§T2W MV: T2 weighted multivane, \*\*\*BTfE/SSFP: Balanced turbo field echo/steady-State free precession, †††DWI: Diffusion weighted imaging

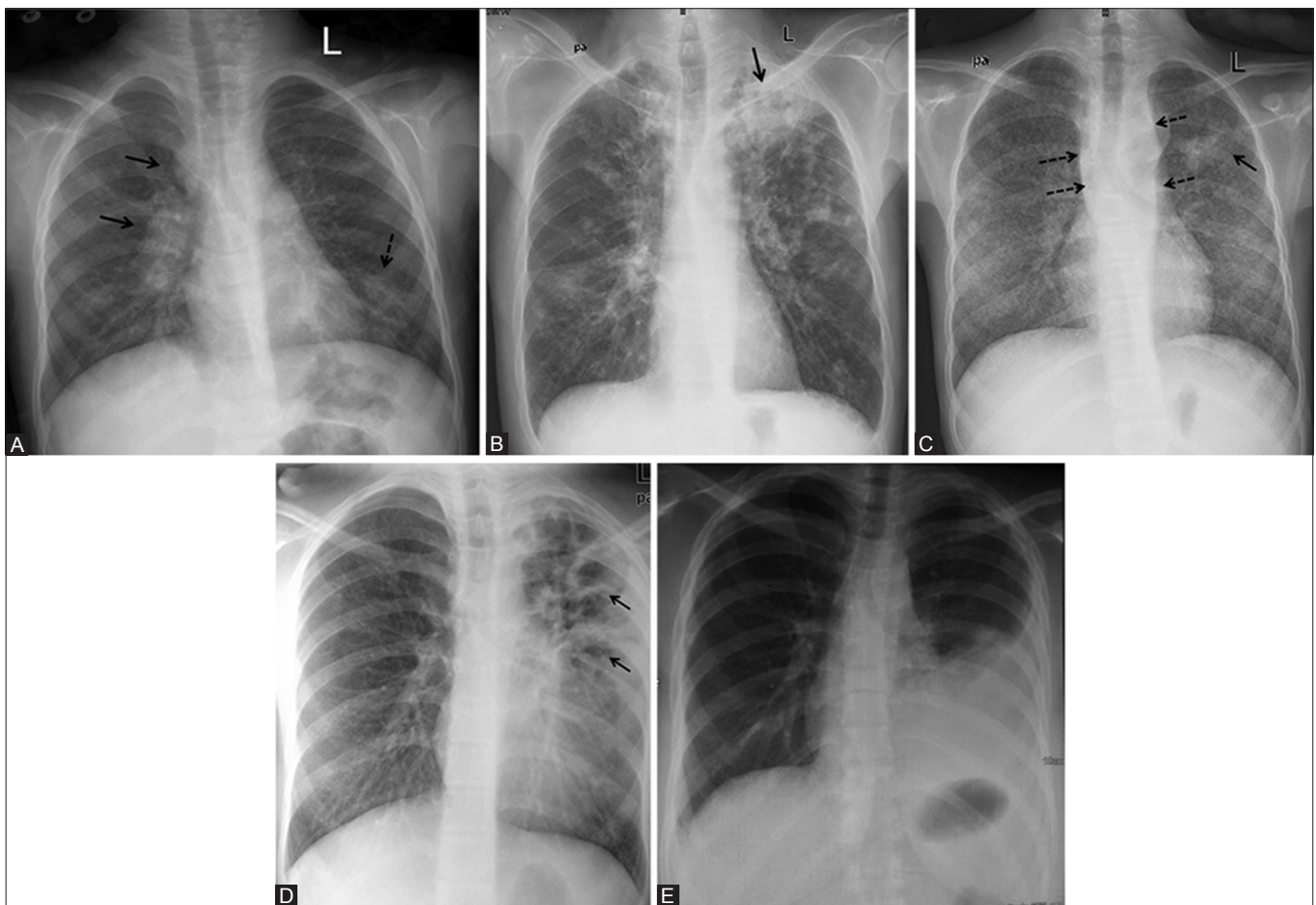


**Figure 3 (A-E):** CXR findings highly suggestive of active TB. (A) CXR showing unilateral (right) paratracheal and hilar lymphadenopathy (solid arrow) with ill-defined air-space opacity in left lower zone (dashed arrow). (B) CXR showing parenchymal consolidation in left upper zone with cavitation (black arrow) and multiple air-space nodules in bilateral upper and mid zones. (C) CXR showing bilateral randomly distributed discrete miliary nodules with consolidation in left upper zone (solid arrow) and bilateral paravertebral shadow (dashed arrow) suggestive of paravertebral abscess. (D) CXR showing multiple thick-walled cavities (solid arrow) with surrounding consolidation in left upper and mid-zone silhouetting left cardiac border. (E) CXR showing unilateral left-sided pleural effusion

group. It is, therefore, advisable to use CT judiciously as a follow-up imaging modality depending upon patient age and clinical manifestations.<sup>[3]</sup> CT may also be used to objectively quantify the involvement of pulmonary parenchyma and airway separately, thereby complimenting the results of PFT.<sup>[3]</sup> Studies have found significant negative correlation between HRCT scoring systems and pulmonary

function parameters, indicative of a decline in lung function with disease progression—a finding of immense prognostic significance.

Last but not the least, CT is required before performing endobronchial ultrasound (EBUS)-guided transbronchial needle aspiration of lymph node in both suspected TB and sarcoidosis. It also allows selection of appropriate site for transbronchial lung biopsy in sarcoidosis. The extent of parenchymal involvement on CT in terms of pattern and distribution can predict the likelihood of positive transbronchial biopsy in sarcoidosis.<sup>[8]</sup>

**Table 2: Imaging recommendations for the diagnosis of suspected sarcoidosis in TB-endemic areas**

Recommendations for CXR
CXR is recommended in all patients
Should serve as entry point for diagnostic algorithm
Frontal radiograph (PA preferable; if not possible, then AP radiograph can be done)
Lateral radiograph is not routinely recommended
To be reported as HS for sarcoidosis, HS for TB, or NS
Recommendations for CT chest
Should be done in all patients labeled as HS or NS for sarcoidosis on CXR and should serve as baseline imaging
Initial CT should be CECT for the comprehensive assessment of mediastinal and hilar lymphadenopathy as well as to exclude other causes
To be reported as HS for TB, HS for sarcoidosis, or NS
HRCT chest without contrast can suffice for follow-up of stages 3 and 4 patients of sarcoidosis

**Endobronchial ultrasound**

EBUS is the newest addition to the available armamentarium of diagnostic imaging modalities in mediastinal lymphadenopathy. EBUS coupled with fine needle aspiration is now a routinely performed procedure for sampling enlarged mediastinal and hilar lymph nodes. Not only does it replace other more invasive procedures like mediastinoscopy but arguably compares with the established diagnostic procedures. Certain studies have compared the endosonographic features of mediastinal lymph nodes in TB and sarcoidosis and found that the sonographic features of heterogeneous echotexture or

**Table 3: CXR findings**

Highly suggestive for active TB	Highly suggestive for active sarcoidosis	Nonspecific
Unilateral hilar/paratracheal lymphadenopathy [Figure 3A and B]	Bilateral symmetric hilar lymphadenopathy in a asymptomatic patient, or in patient with features of Lofgren syndrome or Heerfordt syndrome, or with supportive laboratory data [Figure 4A]	Asymmetric, patchy, multifocal airspace opacities, especially in lower zones [Figure 5A]
With or without ipsilateral parenchymal lesion [Figure 3A and B]	Bilateral perihilar opacities/discrete interstitial perihilar nodules [Figure 4B]	Air space/indeterminate nodules [Figure 5B]
Miliary nodules [Figure 3C]		Thin-walled cavities [Figure 5C]
Cavities with surrounding consolidation/thick walls. Especially in upper and mid zones [Figure 3D]		Equivocal paratracheal stripe widening/hilar enlargement [Figure 5D and E]
Pleural effusion (unilateral) [Figure 3E]		

**Table 4: CT findings**

Highly suggestive for active TB	Highly suggestive for active sarcoidosis	Nonspecific
Airspace nodules/centrilobular nodules (especially tree-in-bud nodules)/clustered nodules especially in bilateral upper lobes, right middle lobe, lingula, superior segment any lower lobe [Figure 6A]	Perilymphatic distribution of micronodules (in subpleural/peribronchovascular/along interlobular septa) in bilateral upper, right middle, and lingular lobes [Figure 7A]	Centrilobular nodules/consolidation in other NS lung segments [Figure 8A and B]
Consolidation in above-mentioned regions with ipsilateral lymph node enlargement [Figure 6B]	Peribronchovascular ill-defined consolidation in upper and middle lobes bilaterally [Figure 7B]	Ground glass opacities [Figure 8C]
Miliary nodules [Figure 6C]	Multiple and bilateral coalescent interstitial nodules [Figure 7C]	Septal thickening/linear opacities
Thick-walled cavity. Cavity with surrounding consolidation [Figure 6D]	-	-
Enlarged mediastinal lymph nodes showing peripheral rim enhancement (due to central necrosis) or heterogeneous enhancement	Enlarged bilateral hilar and right paratracheal lymph nodes	Borderline enlarged discrete lymph nodes with homogeneous enhancement or preserved perinodal fat
Conglomeration of lymph nodes or obscuration of perinodal fat [Figure 6E]	Well-defined, discrete, homogenous, non-coalescent lymph nodes [Figure 7D-F]	Involvement of left paratracheal, subcarinal, aortopulmonary window, and prevascular region lymph nodes [Figure 8D]
Effusion/empyema with split pleura sign [Figure 6F]		

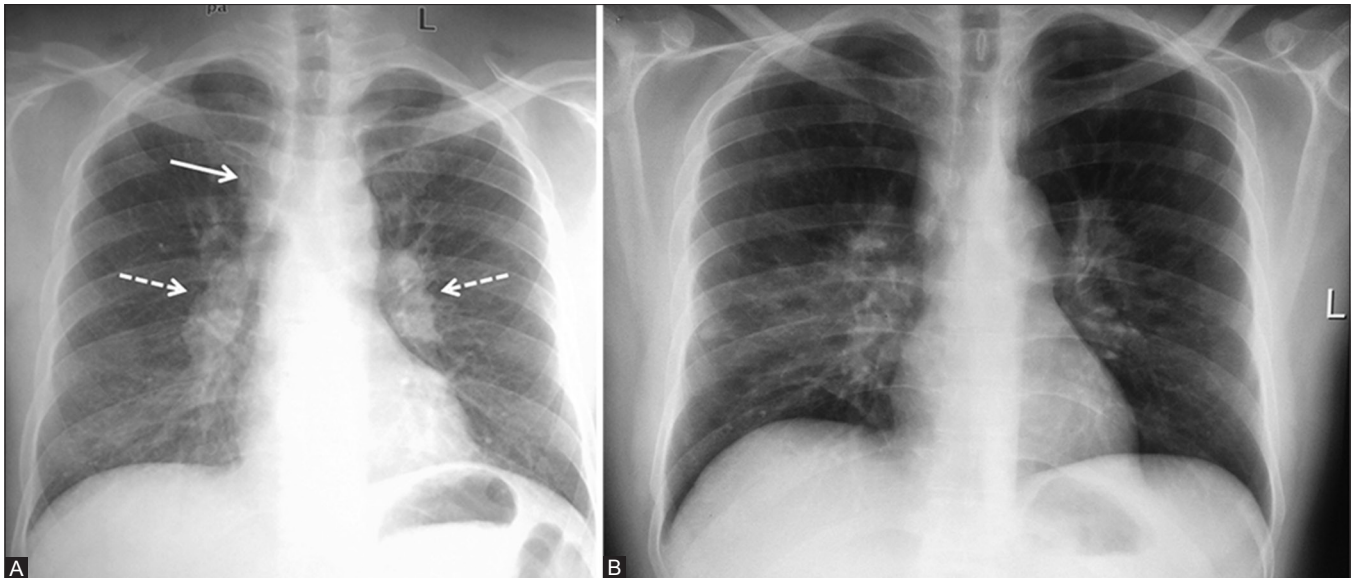


**Figure 4 (A and B):** CXR findings highly suggestive of active sarcoidosis. (A) CXR showing bilateral symmetric hilar and right paratracheal lymphadenopathy. (B) CXR showing bilateral hilar lymphadenopathy with perihilar interstitial nodules, predominantly in upper and mid-zones

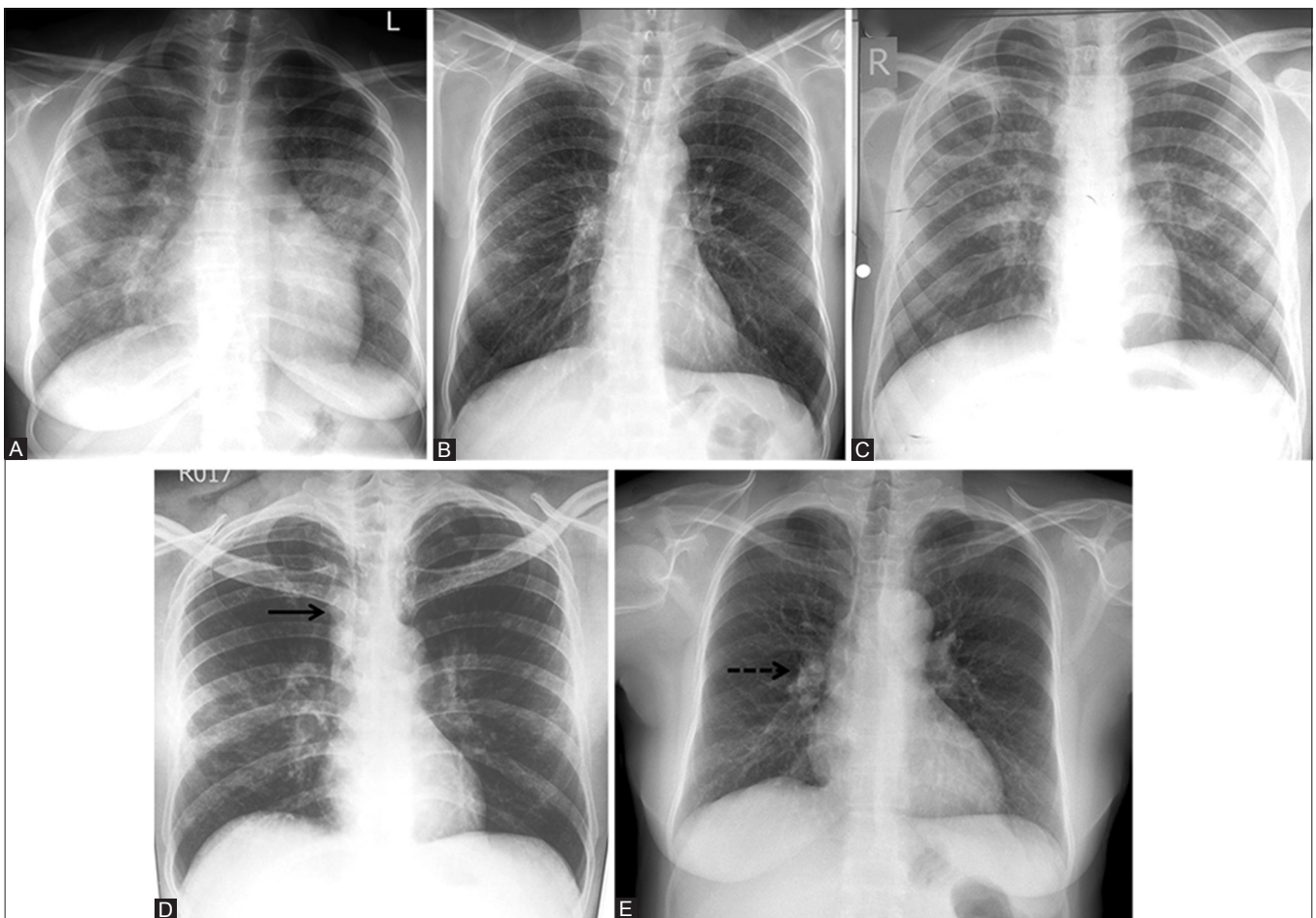


**Figure 5 (A-E):** NS imaging features on CXR. (A) CXR showing patchy, multifocal air-space opacities in bilateral mid and lower zones. (B) CXR showing ill-defined indeterminate nodules in right mid and lower zones. (C) CXR showing a thin-walled cavity in right upper zone with scattered discrete nodules in bilateral mid-zones. (D) CXR showing equivocal paratracheal stripe widening (*solid arrow*). (E) CXR showing equivocal hilar enlargement (*dashed arrow*)

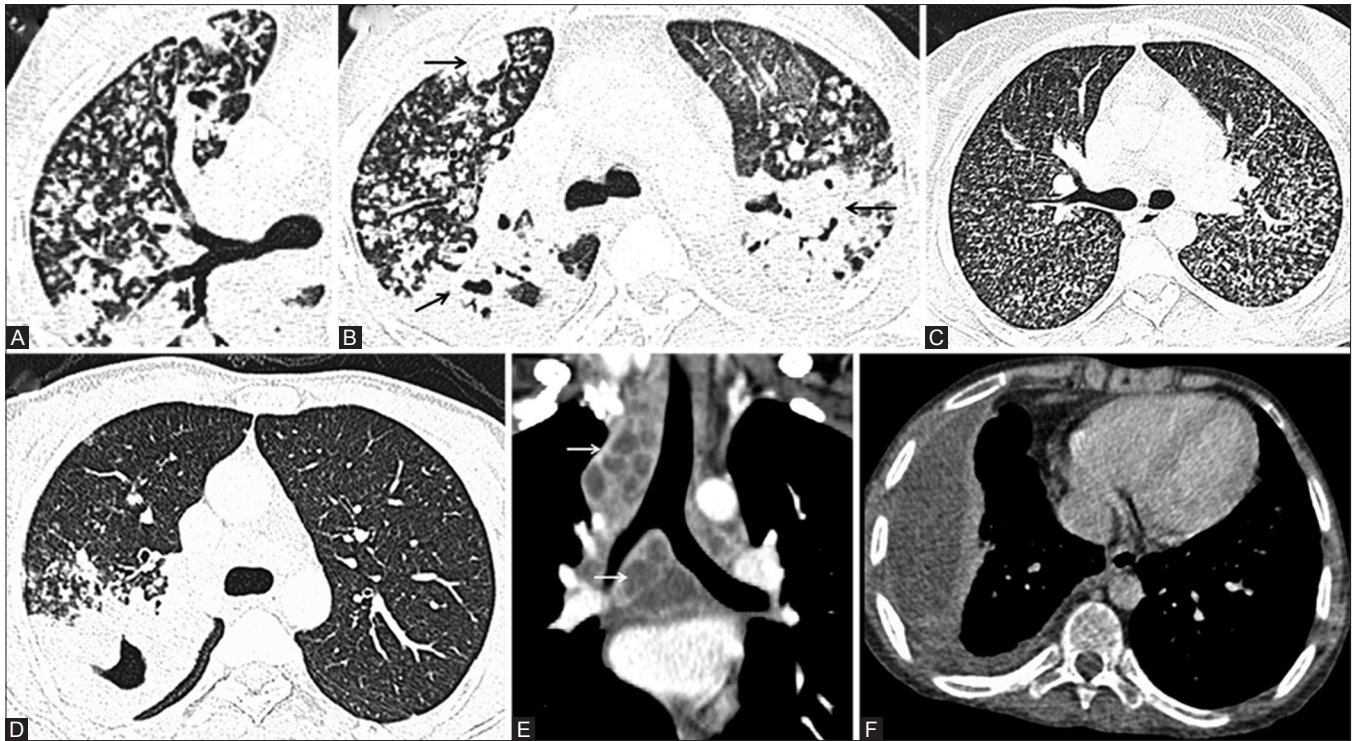


**Figure 6 (A-F):** CT features highly suggestive of active TB. (A) CT chest (lung window) showing centrilobular nodules in tree-in-bud pattern involving right upper lobe and superior segment of right lower lobes. (B) CT (lung window) showing consolidation in bilateral upper lobes and superior segment of right lower lobe (*black arrow*). (C) CT chest (lung window) showing randomly distributed miliary nodules in bilateral lung fields. (D) CT chest (lung window) showing thickwalled cavity with surrounding consolidation in right upper lobe. Extensive centrilobular nodules are noted in adjacent lung parenchyma. (E) Coronal reformatted image of CECT chest showing conglomerate lymph nodes in right upper and lower paratracheal and subcarinal region with obscuration of perinodal fat (*white arrow*). (F) CECT chest showing right-sided empyema with split pleura sign. Note made of volume loss in right hemithorax with crowding of ribs

coagulative necrosis within the lymph nodes are fairly specific for TB and along with a positive tuberculin skin test, these features strongly favor a diagnosis of TB over sarcoidosis.<sup>[9]</sup>

#### Magnetic resonance imaging

MRI is yet another addition to the available imaging modalities for the evaluation of suspected sarcoidosis/TB. With the availability of newer technical innovations in performing MRI of the thorax, its applications in chest imaging have widened. Presence of necrosis is an important differentiating feature between TB and sarcoidosis. MRI has a greater sensitivity to gadolinium than CT has for iodine, and thus contrast-enhanced (CE) MR can accurately detect subtle enhancement and necrosis. MRI also provides multiple paradigms for detection of necrosis: signal detection on T2 weighted (T2W) sequence, enhancement pattern, and diffusion characteristics [Figure 2]. Role of MRI in TB is described as a problem-solving modality to better evaluate mediastinal lymph nodes and assess disease activity in cases of mediastinal nodes/fibrosis.<sup>[5]</sup> Conventional sequences (T1 and T2W images) should be combined with diffusion weighted imaging (DWI) and subtracted CE imaging for optimal evaluation.

Previously, lung parenchyma could not be adequately evaluated with MRI because of paucity of proton in lung parenchyma as well as significant susceptibility artifacts from air-filled lung. But recent technical advances in MR image acquisition and processing have made MR evaluation of pulmonary parenchyma feasible.<sup>[10]</sup> Chung *et al.*<sup>[11]</sup> in their study on 29 subjects of sarcoidosis showed good correlation between MRI and CT in scoring gross parenchymal opacification and reticulation with least agreement in case of pulmonary nodules attributed to the lower inherent spatial resolution of MRI. Agreement was also found to be more in upper lobe disease as opposed to lower lobe disease due to motion artifacts generated by diaphragmatic movements and cardiac pulsation.

Studies in TB have shown that MRI is comparable to CT for identifying morphological pulmonary changes; and that MRI is superior to CT regarding tissue characterization. Furthermore, based on lesion signal intensity, MRI could differentiate the exudative stage of lung TB from the relatively acellular fibrotic stage because of the relatively “short T2” in fibrotic tissues.<sup>[12]</sup>

Recent studies have used gadolinium enhancement characteristics to assess pulmonary fibrosis in sarcoidosis

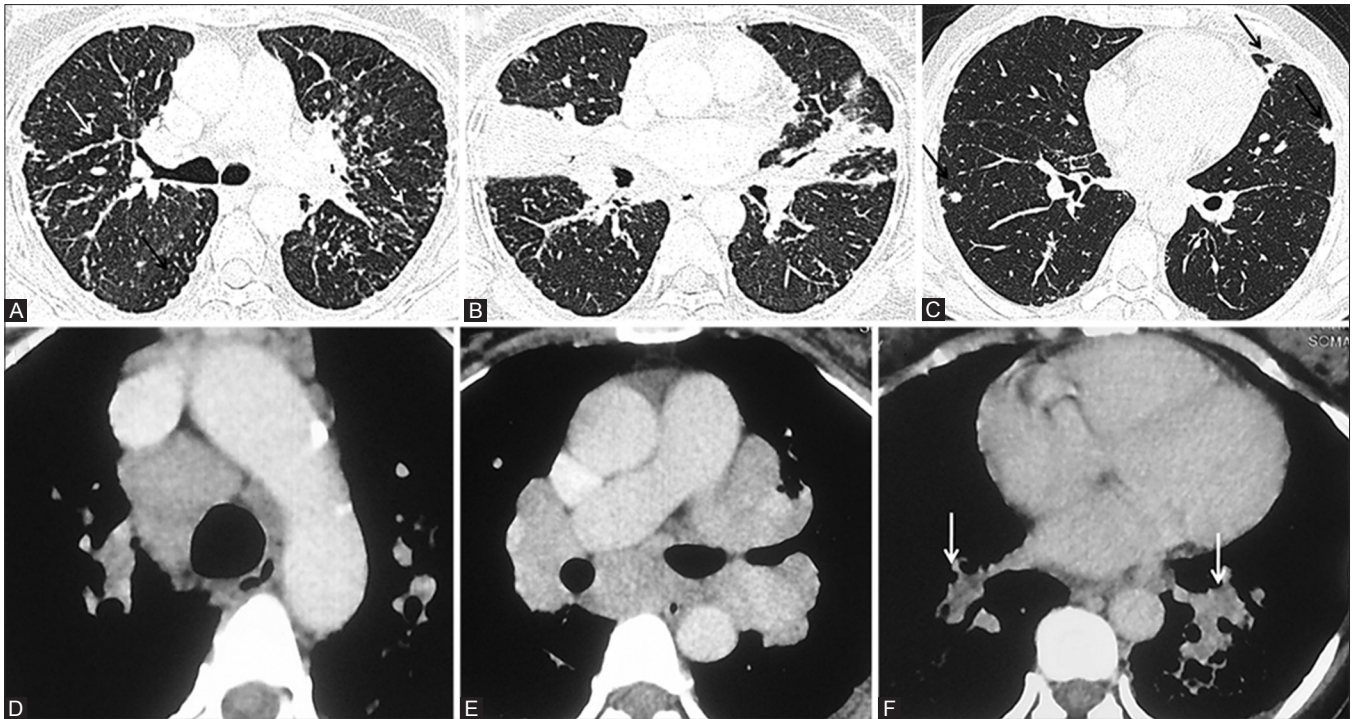


**Figure 7 (A-F):** CT features highly suggestive of active sarcoidosis. (A) CT chest (lung window) showing perilymphatic distribution of micronodules in subpleural (*black arrow*)/peribronchovascular (*white arrow*)/along interlobular septa (*dashed arrow*) in bilateral upper lobes. (B) CT chest (lung window) showing peribronchovascular ill-defined consolidation in upper and middle lobes bilaterally. (C) CT chest (lung window) showing multiple and bilateral coalescent interstitial nodules (*black arrow*). (D-F). Coned down axial CECT chest images showing discrete homogeneous, non-coalescent enlarged bilateral right paratracheal, bilateral hilar, and bronchopulmonary lymph nodes (*white arrow*)

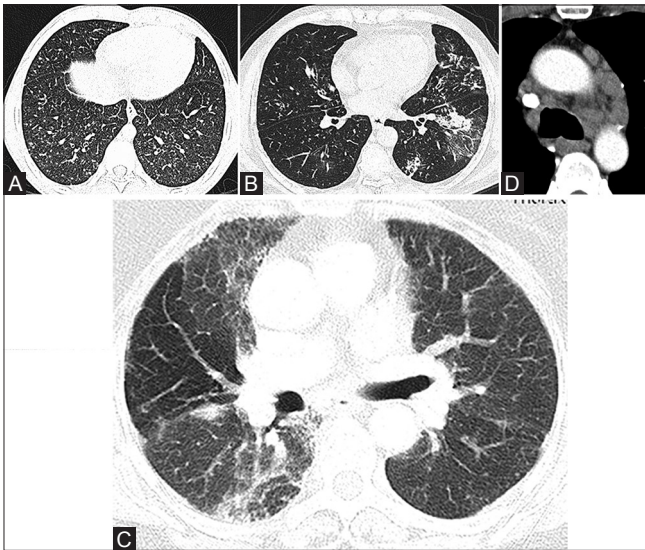


**Figure 8 (A-D):** NS imaging features on CT. (A) CT chest (lung window) showing ill-defined centrilobular nodules in bilateral lower lobes. (B) CT chest (lung window) showing patchy areas of consolidation and ground glass opacity in left lower lobe with scattered centrilobular nodules. (C) CT chest (lung window) showing scattered areas of ground glass opacities in bilateral upper lobes. (D) Coned down axial CECT image showing borderline enlarged discrete lymph nodes in prevascular and aortopulmonary window

as opposed to its anatomical depiction on HRCT in terms of traction bronchiectasis, honeycombing, and reticulation. In their recently published data, Darragh Brady *et al.*<sup>[13]</sup>

used a segmented inversion-recovery turbo FLASH MR sequence with individual pulmonary blood pool nulling to detect fibrotic pulmonary sarcoid. Mean signal intensity in fibrotic lung parenchyma of sarcoid patients was found to be significantly higher ( $46.3 \pm 36.2$ ) as compared to normal lung parenchyma ( $11.1 \pm 2.0$ ,  $P < 0.001$ ). Late enhanced MRI showed significant correlation with HRCT in detecting the extent of pulmonary fibrosis but not fine reticulations or honeycombing. These findings can have significant clinical implications especially in the face of growing concern associated with ionizing radiation, and sarcoidosis being a disease of the young requiring repeated imaging. A multiplanar and multisequence protocol consisting of breath-hold and free breathing sequences is preferred.<sup>[11,14]</sup> Fat-saturated sequences are an essential component of the protocol as they enhance the conspicuity of fluid as well as ghosting artifact of chest wall<sup>[12]</sup> (STIR and T2W multivane fat suppressed in the suggested protocol). Fast sequences (HASTE) with short acquisition times are recommended.<sup>[14]</sup> TruFISP enables study of respiratory mechanics and noncontrast evaluation of mediastinal vessels.<sup>[11]</sup> The examination should also include CE sequences (T1 DIXON) and DWI to complete the assessment of mediastinal lymph nodes, pulmonary nodules, and masses.<sup>[14]</sup> Based on the available literature and institutional experience, the following MR protocol is suggested for the evaluation of suspected sarcoidosis or tuberculosis [Table 1].

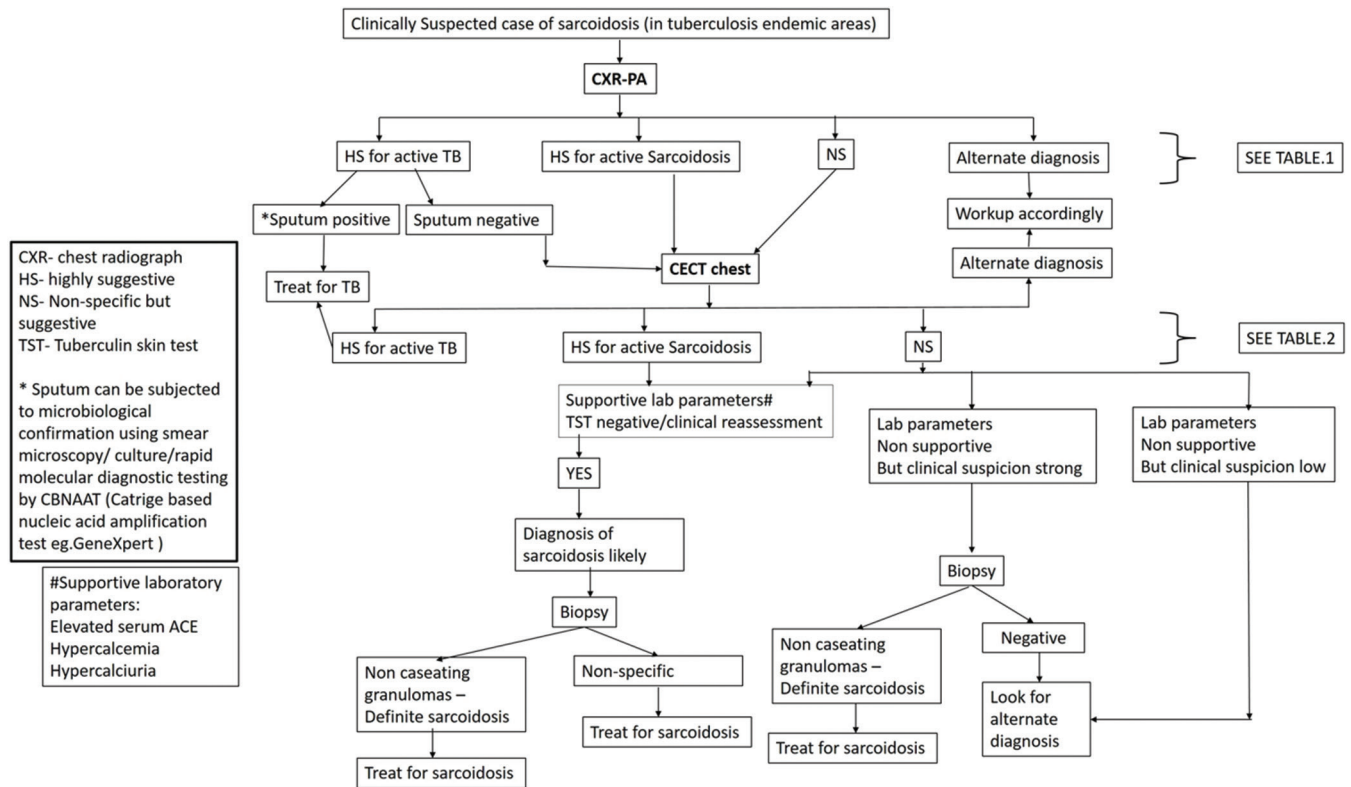


**Figure 9:** Imaging-based algorithm for evaluation of clinically suspected case of sarcoidosis in TB-endemic region

**Positron emission tomography (PET)**

F-18 fluorodeoxyglucose (FDG) PET/CT scan shows tracer uptake in areas of active inflammation in sarcoidosis, which has been used to identify occult site of involvement and suitable sites for biopsy.<sup>[15,16]</sup> In addition, it also enables assessment of active inflammatory sarcoidosis in patients with chronic persistent symptoms, potentially predicting the reversible stage of disease as well as monitoring the response to corticosteroid treatment.<sup>[17,18]</sup> This modality has particularly been useful in assessment of active extrathoracic sites of sarcoidosis such as liver, spleen, retroperitoneal lymph nodes, and myocardium.<sup>[17]</sup>

Active TB shows increased uptake with high standardized uptake values and may pose as a cancer mimic. PET may help in assessing the disease activity and response to therapy in cases of proven TB. Although it is not specific for TB, FDG PET/CT can guide biopsy from active sites, assess complete disease extent, and detect occult distant involvement.<sup>[3]</sup>

Widespread use of this modality is, however, marred by its non-specificity as similar positive uptake may be shown by malignancy or other active inflammatory conditions, the excessive radiation burden, and economic considerations.<sup>[17]</sup> Hence, PET/CT does not feature in the routine diagnostic algorithm for evaluation of sarcoidosis or TB.

**Imaging Recommendations**

The authors, hereby, wish to conclude by suggesting the imaging recommendations for diagnosis of suspected sarcoidosis in TB-endemic regions [Table 2], and imaging findings considered to be highly suggestive of sarcoidosis, TB, or non-specific [Tables 3 and 4, Figures 3-8] followed by an imaging-based algorithm [Figure 9].

**Financial support and sponsorship**  
 Nil.

**Conflicts of interest**

There are no conflicts of interest.

**References**

1. Siltzbach LE. Sarcoidosis: Clinical features and management. *Med Clin North Am* 1967;51:483-502.
2. Hillerdal G, Nöu E, Osterman K, Schmekel B. Sarcoidosis: Epidemiology and prognosis—a 15-year European study. *Am Rev Respir Dis* 1984;130:29-32.
3. Greco FG, Spagnolo P, Muri M, Paladini I, Chizzolini F, Piciocchi S, et al. The value of chest radiograph and computed tomography in pulmonary sarcoidosis. *Sarcoidosis Vasc Diffuse Lung Dis* 2014;31:108-16.
4. Kumar A, Gupta D, Nagaraja SB, Singh V, Sethi GR, Prasad J, et al. Updated current (2012) national guidelines for paediatric tuberculosis in India. *J Indian Med Assoc* 2012;110:840-3.



5. Bhalla AS, Goyal A, Guleria R, Gupta AK. Chest tuberculosis: Radiological review and imaging recommendations. *Indian J Radiol Imaging* 2015;25:213-25.
6. Hamper UM, Fishman EK, Khouri NF, Johns CJ, Wang KP, Siegelman SS. Typical and atypical CT manifestations of pulmonary sarcoidosis. *J Comput Assist Tomogr* 1986;10:928-36.
7. Nunes H, Brillet PY, Valeyre D, Brauner MW, Wells AU. Imaging in sarcoidosis. *Semin Respir Crit Care Med* 2007;28:102-20.
8. de Boer S, Milne DG, Zeng I, Wilsher ML. Does CT scanning predict the likelihood of a positive transbronchial biopsy in sarcoidosis? *Thorax* 2009;64:436-9.
9. Dhooria S, Agarwal R, Aggarwal AN, Bal A, Gupta N, Gupta D. Differentiating tuberculosis from sarcoidosis by sonographic characteristics of lymph nodes on endobronchial ultrasonography: A study of 165 patients. *J Thorac Cardiovasc Surg* 2014;148:662-7.
10. Kauczor HU, Ley-Zaporozhan J, Ley S. Imaging of pulmonary pathologies: Focus on magnetic resonance imaging. *Proc Am Thorac Soc* 2009;6:458-63.
11. Chung JH, Little BP, Forssen AV, Yong J, Nambu A, Kazlouski D, *et al.* Proton MRI in the evaluation of pulmonary sarcoidosis: Comparison to chest CT. *Eur J Radiol* 2013;82:2378-85.
12. Rizzi EB, Schinina V, Cristofaro M, Goletti D, Palmieri F, Bevilacqua N, *et al.* Detection of pulmonary tuberculosis: Comparing MR imaging with HRCT. *BMC Infect Dis* 2011;11:243.
13. Brady D, Lavelle LP, McEvoy SH, Murphy DJ, Gallagher A, Gibney B, *et al.* Assessing fibrosis in pulmonary sarcoidosis: Late-enhanced MRI compared to anatomic HRCT imaging. *QJM* 2016;109:257-64.
14. Hochegger B, de Souza VV, Marchiori E, Irion KL, Souza Jr AS, Elias Junior J, *et al.* Chest magnetic resonance imaging: A protocol suggestion. *Radiol Bras* 2015;48:373-80.
15. Braun JJ, Kessler R, Constantinesco A, Imperiale A. 18F-FDG PET/CT in sarcoidosis management: Review and report of 20 cases. *Eur J Nucl Med Mol Imaging* 2008;35:1537-43.
16. Teirstein AS, Machac J, Almeida O, Lu P, Padilla ML, Iannuzzi MC. Results of 188 whole-body fluorodeoxyglucose positron emission tomography scans in 137 patients with sarcoidosis. *Chest* 2007;132:1949-53.
17. Sobic-Saranovic D, Artiko V, Obradovic V. FDG PET imaging in sarcoidosis. *Semin Nucl Med* 2013;43:404-11.
18. Mostard RL, Voo S, van Kroonenburgh MJ, Wijnen PA, Nelemans PJ, Drent M, *et al.* Inflammatory activity assessment by F18 FDG-PET/CT in persistent symptomatic sarcoidosis. *Respir Med* 2011;105:1917-24.